



UNIVERSITY
OF TRENTO

DIPARTIMENTO DI INGEGNERIA E SCIENZA DELL'INFORMAZIONE

38123 Povo – Trento (Italy), Via Sommarive 14
<http://www.disi.unitn.it>

SYNTHESIS OF A PRE-FRACTAL DUAL-BAND MONOPOLAR
ANTENNA FOR GPS APPLICATIONS

R. Azaro, F. De Natale, E. Zeni, M. Donelli, and A. Massa

January 2011

Technical Report # DISI-11-076

Synthesis of a Pre-Fractal Dual-Band Monopolar Antenna for GPS Applications

Renzo Azaro, Francesco De Natale, Massimo Donelli, Edoardo Zeni, and Andrea Massa

Department of Information and Communication Technologies,
University of Trento, Via Sommarive 14, I-38050 Trento - Italy

Tel. +39 0461 882057, Fax +39 0461 882093

E-mail: {*andrea.massa, francesco.denatale*}@*ing.unitn.it*,

{*renzo.azaro, massimo.donelli, edoardo.zeni*}@*dit.unitn.it*

Web-page: <http://www.eledia.ing.unitn.it>

Synthesis of a Pre-Fractal Dual-Band Monopolar Antenna for GPS Applications

Renzo Azaro, Francesco De Natale, Massimo Donelli, Edoardo Zeni, and Andrea Massa

Abstract

In this letter, the design of a monopolar dual-band antenna operating in the $L1$ and $L2$ *GPS* bands is presented. The pre-fractal geometry of the antenna has been synthesized by means of a Particle Swarm algorithm for optimizing the values of the electrical parameters within the specifications. For a general assessment, some selected results of numerical simulations are shown and some comparisons between numerical data and experimental measurements are presented.

Key-words:

Antennas Synthesis, Pre-fractal Antennas, Multi-band Antennas, Microstrip Antennas, GPS, Particle Swarm Optimizer.

1 Introduction

Nowadays, the development of electronic devices employing various wireless standards for the data exchange and operating in different frequency bands requires the use of multi-band components. In such a framework, the antenna synthesis is a critical task since the design and the development of a single radiator working in two or more frequency bands is generally not easy especially when dimensional/geometrical constraints on the structure are imposed.

Elementary wire antennas (e.g., finite dipoles and monopoles) work in several frequency bands related to the resonances of the structure. However, such multiple working frequencies are usually harmonic and the corresponding electrical parameters (i.e., $VSWR$ and gain) vary depending on the resonance frequency.

On the other hand, standard techniques for the development of multiband wire antennas consider the insertion of reactive loads in the antenna structure for obtaining and controlling multiple (non harmonic, as well) resonant frequencies. In recent years, such an issue has been also addressed by exploiting the properties of fractals geometries and synthesizing both the antenna geometry and loads values and positions by means of suitable optimization algorithms [1]. As a matter of fact, the use of fractal structures or more precisely pre-fractal geometries (i.e., characterized by a finite number of fractal iterations) for the antennas synthesis has been proven to be very effective for achieving a dimensional miniaturization and an enhanced bandwidth [2][3], even though an increase of the effective bandwidth of the antenna turns out in a reduction of the radiation efficiency at resonant frequencies [4][5][6]. Furthermore, some interesting applications have been recently presented in literature [7][8] further confirming the positive features of pre-fractal structures in the framework of antenna synthesis. However, it should be pointed out that classical pre-fractal geometries usually present an harmonic frequency behavior rather than a multiband behavior as observed in [7] where Koch-like structures have been considered.

A possible solution for tuning and controlling the spacing between the working frequencies of a fractal antenna is based on the perturbation of the fractal geometry by adding some degrees of freedom in the synthesis process. Towards this end, some attempts have been

performed by considering a Sierpinski fractal antenna and perturbing the characteristic scale factor of the fractal shape [9]. According to the idea of adding other degrees of freedom but unlike the approach proposed in [9], this letter presents a preliminary result concerned with a pre-fractal Koch-like dual-band antenna printed on a dielectric substrate and operating in the $L1$ and $L2$ bands of the Global Positioning System (GPS). The design of the fractal geometry is carried out through a numerical procedure based on a particle swarm optimizer (PSO) [10][11][12], which optimizes the parameters of the pre-fractal geometry (lengths, widths, and orientation angles of the printed segments) avoiding the insertion of any lumped load as in [1] to obtain a multi-band behavior. In order to assess the effectiveness of the design procedure and the characteristics of the synthesized antenna, the obtained numerical results are compared with the measurements from an experimental prototype.

2 Dual-Band GPS Antenna Design and Optimization

The design of the dual-band GPS monopolar antenna has been formulated in terms of an optimization problem by defining and imposing suitable constraints both on the gain values and about the impedance matching at the input port in the $L1$ and $L2$ frequency bands of the GPS system (centered at $f_{L1} = 1227.60 MHz$ and $f_{L2} = 1575.42 MHz$, respectively). As far as the antenna for the GPS receiver is concerned, radiation characteristics that guarantee a hemispherical coverage have been assumed. Moreover, a voltage-standing-wave-ratio ($VSWR$) lower than 1.8 in both the working frequency bands (i.e., a reflected power lower than 10 % of the incident power) has been required at the input port the antenna. Such constraints have been chosen taking into account the following specification of a commercial GPS receiver: (a) gain values greater than $G_{min} = 3.0 dBi$ at $\theta = 0$ and greater than $G_{min} = -4.0 dBi$ at $\theta = 70$, respectively; (b) the maximum value of the $VSWR$ equal to 2.0. Since the first stage (connected to the antenna) of each GPS receiving system is generally a low noise preamplifier because of the low intensity of the GPS signals at the earth surface, then a better impedance matching has been imposed by decreasing the maximum $VSWR$ value from 2.0 up to $VSWR_{max} = 1.8$ in order to allow improved performances. Concerning the geometrical constraints, the antenna has

been also required to belong to a physical platform of dimensions $10 \times 16 \text{ cm}^2$.

By considering a microstrip structure printed on a planar dielectric substrate, the parameters to be optimized were the fractal geometry and the width and the length of each fractal segment. As far as the general shape of the generating antenna is concerned, a Koch-like geometry derived from the Koch curve described in [1] and [7] has been used. According to the notation used in [1], the antenna has been generated from the Koch curve by repeatedly applying the so-called Hutchinson operator until the stage $i = 2$, in order to obtain a radiating device with two resonant frequencies. In general, the antenna structure at i -th stage is uniquely determined by: (a) a set of segment lengths $s_{i,j}$, i being the index of the fractal stage and j ($j = 1, \dots, 4^i$) indicates the j -th segment at the i -th stage; (b) a set of segment widths $w_{i,j}$; (c) a set of angles $\Theta_{h,q}$, $h = 1, \dots, 2^i$ and $q = 1, 2$ being $\Theta_{h,1} = \Theta_{h,2}$. As an example, the descriptive parameters $s_{i,j}$ and $\Theta_{h,q}$ of the Koch-like curve at $i = 1$ and $i = 2$ are reported in Fig. 1(a) and in Fig. 1(b), respectively. In order to synthesize the GPS dual-band antenna, the $i = 2$ stage has been considered and, in order to satisfy the project guidelines, the unknown descriptive parameters of the antenna have been optimized by minimizing the cost function Ω defined in terms of the least-square difference between requirements and estimated specifications:

$$\Omega(\underline{\gamma}) = \min \left\{ \varphi(\underline{\gamma}_i); i = 2 \right\} \quad (1)$$

being

$$\begin{aligned} \varphi(\underline{\gamma}_i) = & \sum_{m=0}^{M-1} \sum_{n=0}^{N-1} \sum_{t=0}^{T-1} \left\{ \max \left[0, \frac{G_{\min}\{t\Delta\theta, n\Delta\phi, m\Delta f\} - \Phi\{t\Delta\theta, n\Delta\phi, m\Delta f\}}{G_{\min}} \right] \right\} + \\ & + \sum_{v=0}^{V-1} \left\{ \max \left[0, \frac{\Psi\{v\Delta f\} - VSWR_{\max}}{VSWR_{\max}} \right] \right\} \end{aligned} \quad (2)$$

where $\underline{\gamma}_i = \{s_{i,j}, w_{i,j}, \Theta_{h,1}; j = 1, \dots, 4^i; h = 1, \dots, 2^i\}$, Δf is the sampling frequency step in the $L1$ and $L2$ bands, $\Delta\theta$ and $\Delta\phi$ are the sampling angular steps of the gain function; $\Phi\{\underline{\gamma}_i\} = \Phi\{t\Delta\theta, n\Delta\phi, m\Delta f\}$ is the gain of the GPS antenna evaluated at $(\theta = t\Delta\theta, \phi = n\Delta\phi, f = m\Delta f)$ and $\Psi\{\underline{\gamma}_i\} = \Psi\{v\Delta f\}$ is the $VSWR$ value at the frequency

$f = m\Delta f$ when the antenna structure is defined by the descriptive array $\underline{\gamma}_i$, $i = 2$.

Besides the electrical constraints, suitable conditions on the overall length and width of the fractal curve have been considered and a penalty has been imposed on some geometric configurations (e.g., having large ratio between width and length of the fractal segment) to avoid the generation of unfeasible structures.

In order to minimize (1) and according to the guidelines reported in [11], a suitable implementation of the *PSO* [13] has been integrated with a pre-fractal generator and a method-of-moments (*MoM*) [14] electromagnetic simulator. Starting from the set of trial arrays $\underline{\gamma}_{i,p}^{(k)}$ (i being the index of the considered fractal stage, i.e. $i = 2$, and k being the trial array index, $p = 1, \dots, P$, and the iteration index, $k = 0, \dots, K$, respectively) iteratively defined by the *PSO*, the pre-fractal generator defines the corresponding antenna structures for computing the corresponding *VSWR* and gain values by means of the *MoM* simulator, which takes into account the presence of the dielectric slab and of the reference ground plane assumed of infinite extent. The iterative process continues until $k = K$ or $\Omega^{opt} \leq \eta$, η being the convergence threshold and $\Omega^{opt} = \min_k \left\{ \min_p \left[\Omega \left(\underline{\gamma}_{i,p}^{(k)} \right) \right] \right\}$.

3 Numerical Simulation and Experimental Validation

The *PSO* implementation adopted in this work considers a population of $P = 8$ trial solutions, a threshold $\eta = 10^{-3}$, and a maximum amount of iterations equal to $K = 2000$. The remaining parameters of the *PSO* have been set referring to the reference literature [11] and according to [13]. As an illustrative example of the iterative synthesis process, Figures 2 and 3 show some representative processing results at various steps. At each step, the structure of the best solution is shown (Fig. 2) as well as the plot of the corresponding *VSWR* function (Fig. 3). As it can be observed, starting from a fully mismatched solution concerned with the structure displayed in Fig. 2(a) ($k = 0$), the solution improves until the final geometry shown in Fig. 2(e) ($k = k_{conv}$) that fits the project specification in terms of both *VSWR* values and gain values at $\theta = 0$ and $\theta = 70$. Furthermore, the synthesized antenna fits the geometrical constraints since its transversal and longitudinal dimensions are equal to $123 [mm]$ along the x -axis and $43 [mm]$ along the y -axis. Concerning the cost function minimization, Figure 4 shows the plot of the

cost function versus the iteration number. As it can be noticed, the optimization required $k_{conv} = 367$ iterations and each iteration taken an amount of *CPU*-time approximately of about 10 *sec* (Pentium IV 1800 *MHz*, 512 *MB* RAM).

As a result of the satisfactory numerical study, an experimental validation has been carried out. The antenna prototype has been built by using a photolithographic printing circuit technology following the geometric guidelines coming from the simulations and pictorially resumed in Fig. 2(e). As far as the *VSWR* experimental measurements are concerned, the antenna prototype (Fig. 5) has been equipped with a *SMA* connector and it has been placed on a reference ground plane with dimensions of $90 \times 140 \text{ cm}^2$. The *VSWR* values have been measured with a scalar network analyzer by placing the antenna inside an anechoic chamber. Computed and measured *VSWR* values have been compared and the results are shown in Figure 6. As it can be observed, there is a good agreement between simulated and measured data, which satisfy the project constraints both in the *L1* frequency band ($VSWR]_{sim} = 1.68$ vs. $VSWR]_{meas} = 1.42$) and in the *L2* frequency band ($VSWR]_{sim} = 1.21$ vs. $VSWR]_{meas} = 1.08$).

In order to asses the effectiveness of the design methodology, the simulated and experimentally-evaluated *VSWR* values are compared in Fig. 7 with those concerned with two quarter-wave monopoles working at the *L1* and the *L2* bands, respectively, and with the values reported in [15] for a GPS dual-band loaded-antenna. Although the synthesized structure presents a *x*-length equal to approximately $\frac{\lambda_1}{2}$, λ_1 being the wavelength at $f_{L1} = 1227.60 \text{ MHz}$, it gives *VSWR* values comparable with those of the corresponding quarter-wave monopoles (for each operating band), but avoiding the use of multiple wired structures or a tuning circuit. Moreover, the *VSWR* behavior turns out to be similar to that in [15] and concerned with a loaded antenna, but without lumped loads.

Finally, Figs. 8(a)-(b) show the simulated gain functions in the horizontal plane ($\theta = 0$) and in a vertical plane ($\phi = 0$), respectively. In order to validate the compliance to the requirements in a realistic configuration, the numerical simulations have been carried out considering a finite ground plane having the same dimensions of that used during *VSWR* measurements ($90 \times 140 \text{ cm}^2$). As expected, the synthesized antenna allows the hemispherical coverage requested by the *GPS* applications. Moreover the gain values at $\theta = 0$ and

at $\theta = 70$ turns out to be greater than specifications ($\Phi \{\theta = 0\} > G_{min} \{\theta = 0\} = 3.0 \text{ dBi}$ and $\Phi \{\theta = 70\} > G_{min} \{\theta = 70\} = -4.0 \text{ dBi}$).

4 Conclusions

The design and optimization of a dual-band pre-fractal *GPS* antenna printed on a dielectric substrate has been described. The antenna structure has been synthesized through a suitable particle swarm algorithm by optimizing the descriptive parameters of a Kock-like pre-fractal geometry in order to comply with the geometrical requirements as well as the electrical constraints in the *L1* and *L2 GPS* frequency bands. A prototype of the dual-band antenna has been built and some comparisons between measured and simulated *VSWR* values have been carried out in order to assess the effectiveness of the optimized antenna as well as (in a preliminary fashion) of the overall synthesis procedure.

Acknowledgements

This work has been supported in Italy by the “Progettazione di un Livello Fisico ‘Intelligente’ per Reti Mobili ad Elevata Riconfigurabilità,” Progetto di Ricerca di Interesse Nazionale - MIUR Project COFIN 2005099984 and by the *Center of REsearch And Telecommunication Experimentations for NETworked communities* (CREATE-NET).

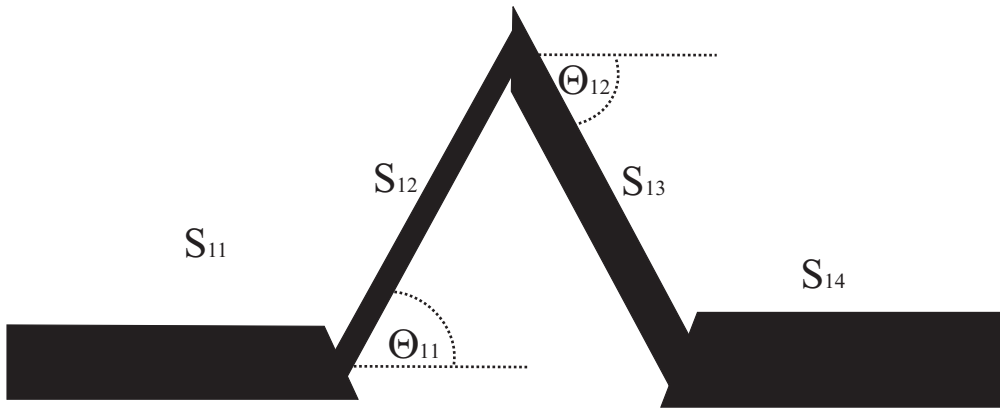
References

- [1] D. H. Werner, P. L. Werner, and K. H. Church, "Genetically engineered multiband fractal antennas," *Electron. Lett.*, vol. 37, pp. 1150-1151, Sep. 2001.
- [2] D. H. Werner and R. Mittra, *Frontiers in electromagnetics*. Piscataway: IEEE Press, 2000.
- [3] J. Gianvittorio and Y. Rahmat-Samii, "Fractals antennas: A novel antenna miniaturization technique, and applications," *IEEE Antennas Propagat. Mag.*, vol. 44, pp. 20-36, Feb. 2002.
- [4] S. R. Best, "A comparison of the resonant properties of small space-filling fractal antennas," *IEEE Antennas Wireless Propagat. Lett.*, vol. 2, pp. 197-200, 2003.
- [5] J. M. González-Arbesù, S. Blanch, J. Romeu, "Are space-filling curves efficient small antennas?," *IEEE Antennas Wireless Propagat. Lett.*, vol. 2, pp. 147-150, 2003.
- [6] J. M. González-Arbesù, J. Romeu, "On the influence of fractal dimension on radiation efficiency and quality factor of self-resonant prefractal wire monopoles," in *Proc. IEEE Antennas Propagat. Symp.*, Jun. 2003.
- [7] C. P. Baliarda, J. Romeu, and A. Cardama, "The Koch monopole: a small fractal antenna," *IEEE Antennas Propagat. Mag.*, vol. 48, pp. 1773-1781, Nov. 2000.
- [8] S. R. Best, "On the performance properties of the Koch fractal and other bent wire monopoles," *IEEE Trans. Antennas Propagat.*, vol. 51, pp. 1292-1300, Jun. 2003.
- [9] C. Puente, J. Romeu, R. Bartoleme, and R. Pous, "Perturbation of the Sierpinski antenna to allocate operating bands," *Electron. Lett.*, vol. 32, pp. 2186-2188, Nov. 1996.
- [10] J. Kennedy, R. C. Eberhart, and Y. Shi, *Swarm Intelligence*. San Francisco: Morgan Kaufmann Publishers, 2001.
- [11] J. Robinson and Y. Rahmat-Samii, "Particle swarm optimization in electromagnetics," *IEEE Trans. Antennas Propagat.*, vol. 52, pp. 397-407, Feb. 2004.

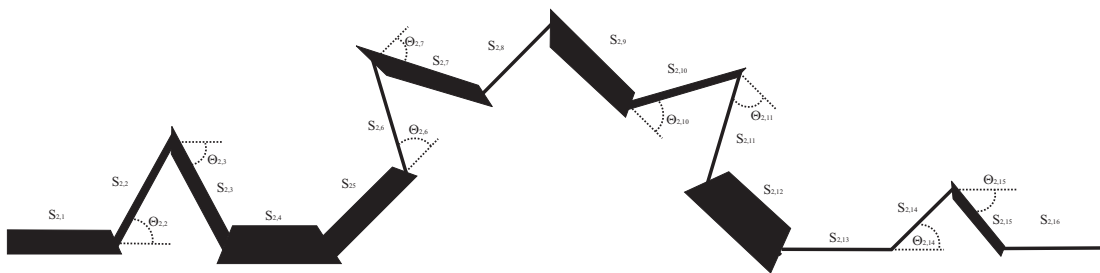
- [12] M. Donelli and A. Massa, "A computational approach based on a particle swarm optimizer for microwave imaging of two-dimensional dielectric scatterers," *IEEE Trans. Microwave Theory Techn.*, vol. 53, pp. 1761-1776, May 2005.
- [13] R. Azaro, F. De Natale, M. Donelli, A. Massa, and E. Zeni, "Optimized design of a multi-function/multi-band antenna for automotive rescue systems," *IEEE Trans. Antennas Propagat.* - Special Issue on "Multifunction Antennas and Antenna Systems," in press Feb. 2006.
- [14] R. F. Harrington, *Field Computation by Moment Methods*. Malabar, Florida: Robert E. Krieger Publishing Co., 1987.
- [15] D. H. Werner and S. Ganguly, "An overview of fractal antenna engineering research," *IEEE Antennas Propagat. Mag.*, vol. 45, pp. 38-57, 2003.

Figure Captions

- **Figure 1.** Descriptive parameters of the Koch-like fractal antenna: (a) $i = 1$ and (b) $i = 2$.
- **Figure 2.** Geometry of the *GPS* dual-band fractal monopole at different iterations of the optimization process: (a) $k = 0$, (b) $k = 10$, (c) $k = 50$, (d) $k = 100$, and (e) $k = k_{conv}$.
- **Figure 3.** Simulated *VSWR* values at the input port of the *GPS* dual-band fractal monopole antenna at different iterations of the optimization procedure.
- **Figure 4.** Behavior of the cost function versus the iteration number.
- **Figure 5.** Photograph of the prototype of the *GPS* dual-band fractal monopole.
- **Figure 6.** *GPS* dual-band fractal monopole: comparison between measured and simulated *VSWR* values.
- **Figure 7.** *GPS* dual-band fractal monopole. Comparison between *PSO*-based synthesis and conventional solutions.
- **Figure 8.** *GPS* dual-band fractal monopole: gain functions calculated on a finite ground plane at (a) the horizontal plane and (b) at the vertical plane ($\phi = 0$).

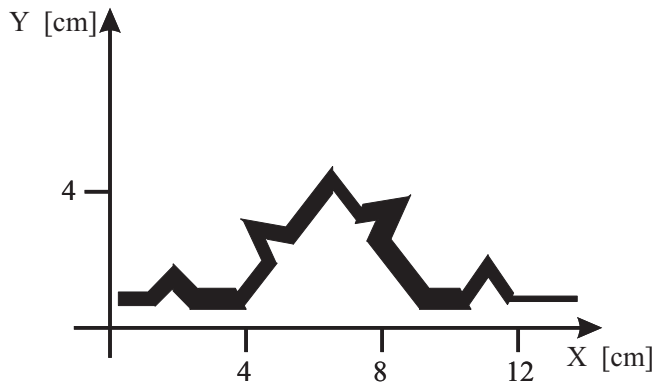


(a)

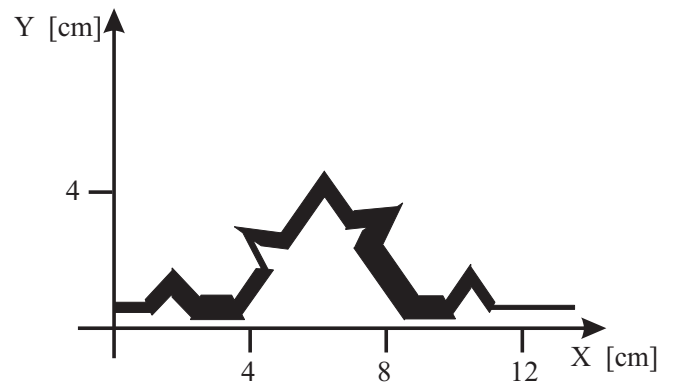


(b)

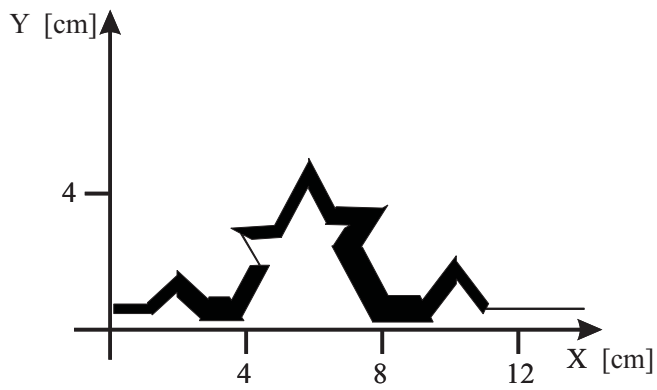
Figure 1 - R. Azaro *et al.*, "Synthesis of a pre-fractal dual-band monopolar ..."



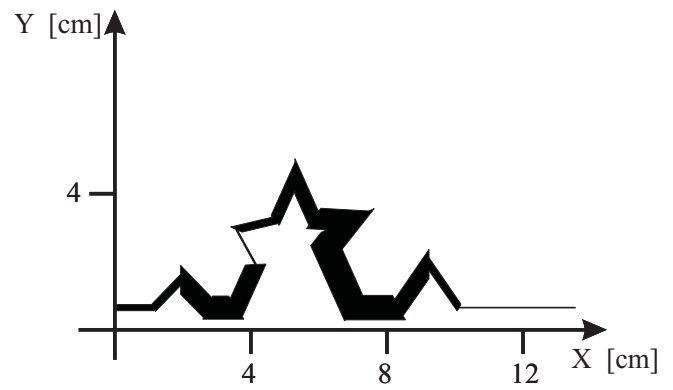
(a)



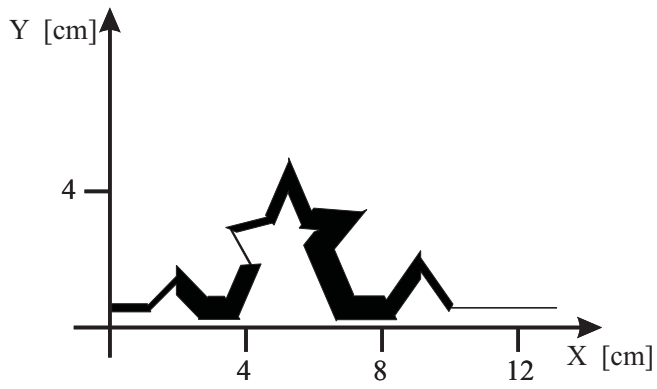
(b)



(c)



(d)



(e)

Figure 2 - R. Azaro *et al.*, "Synthesis of a pre-fractal dual-band mopolar ..."



/home/elede/Ricerca/Sintesi.Antenne.Frattali/Papers/IEEE-AWPL.2006/Fi

Figure 3 - R. Azaro *et al.*, “Synthesis of a pre-fractal dual-band monopolar ...”

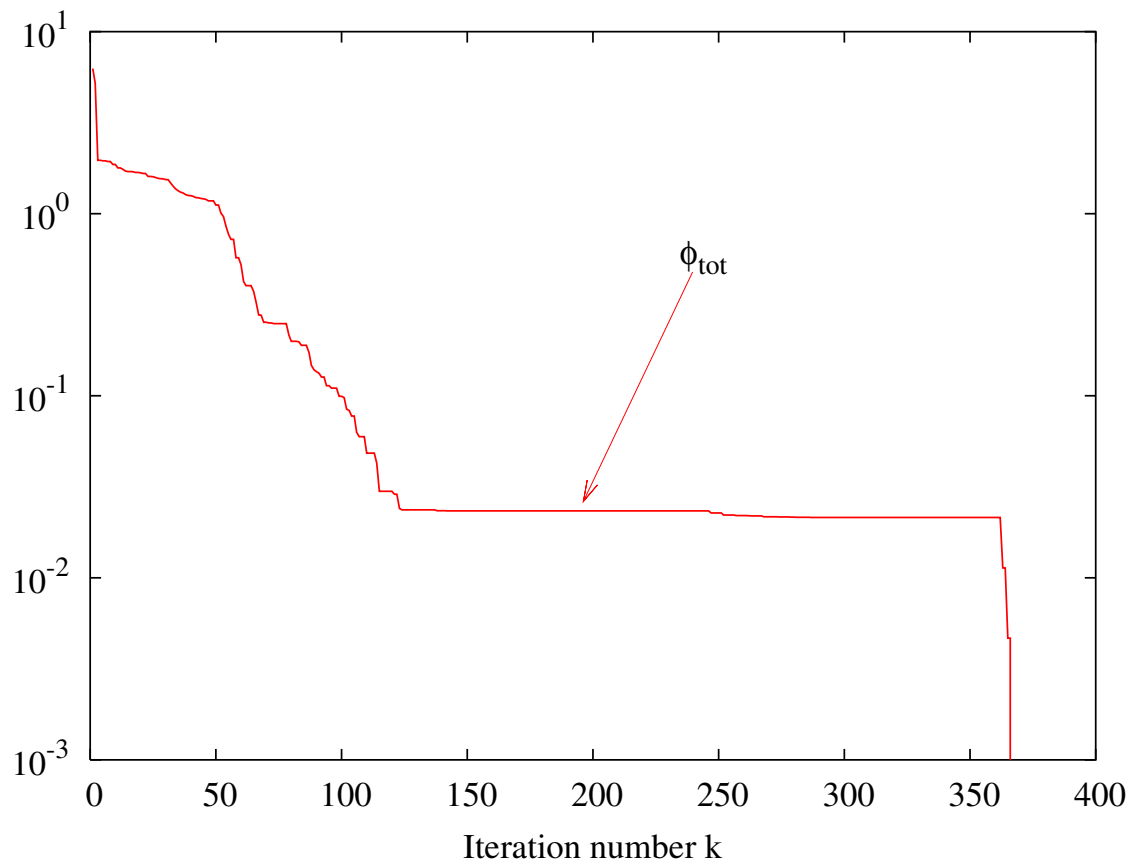


Figure 4 - R. Azaro *et al.*, "Synthesis of a pre-fractal dual-band mopolar ..."



Figure 5 - R. Azaro *et al.*, “Synthesis of a pre-fractal dual-band monopolar ...”

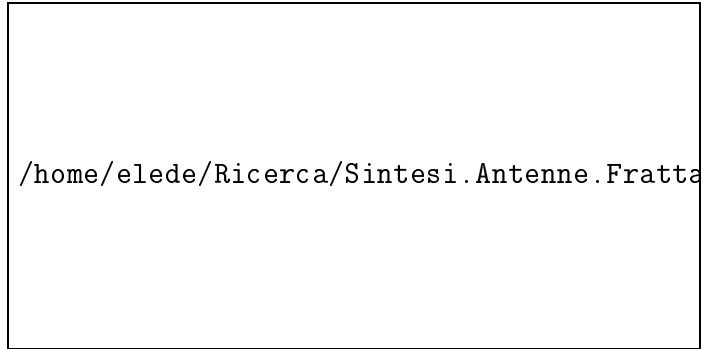


Figure 6 - R. Azaro *et al.*, "Synthesis of a pre-fractal dual-band monopolar ..."

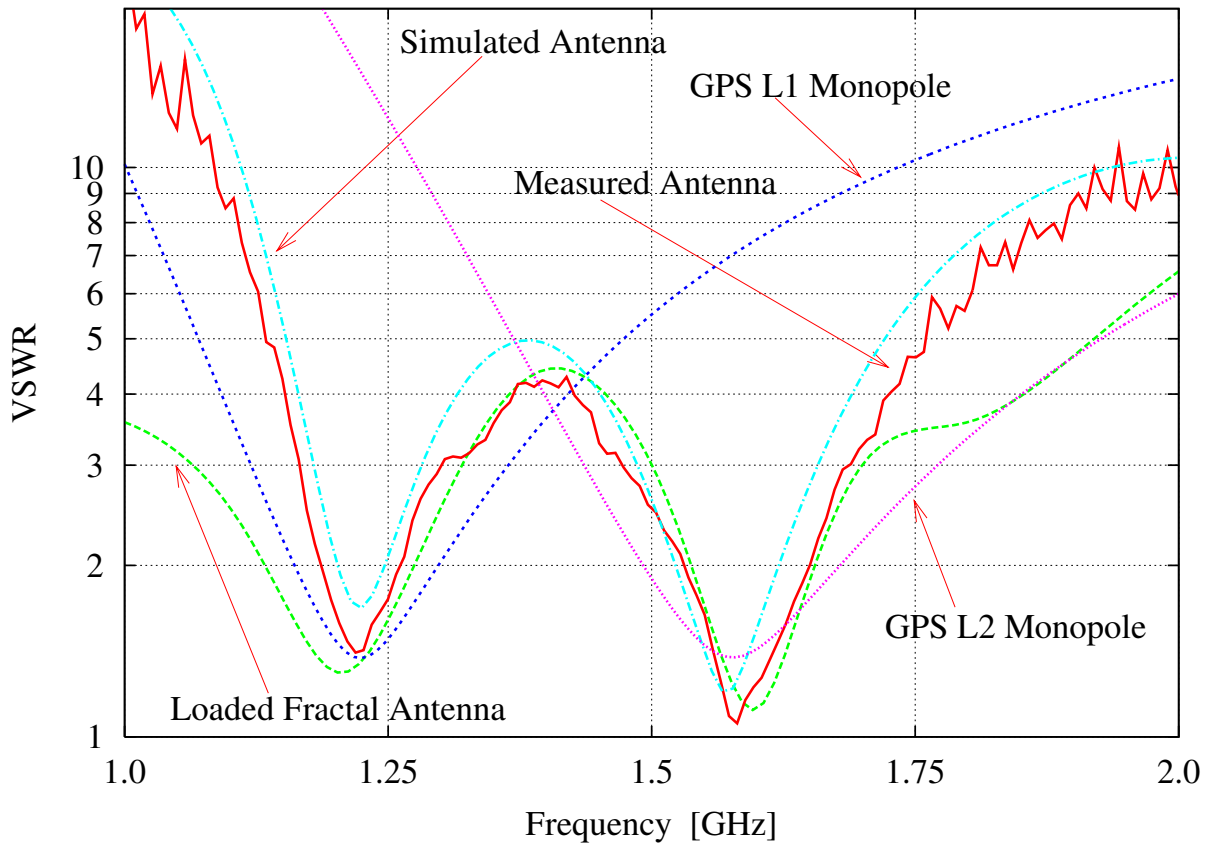
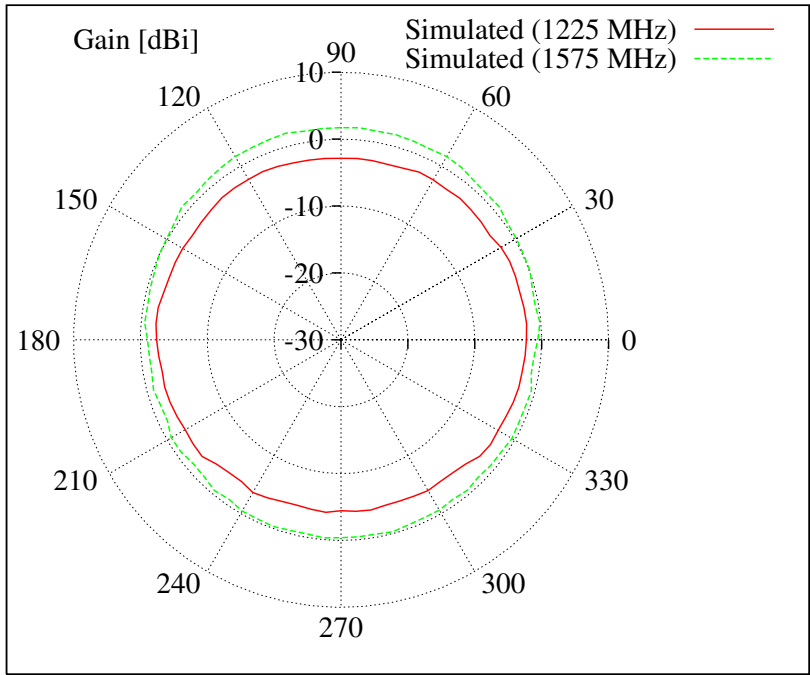
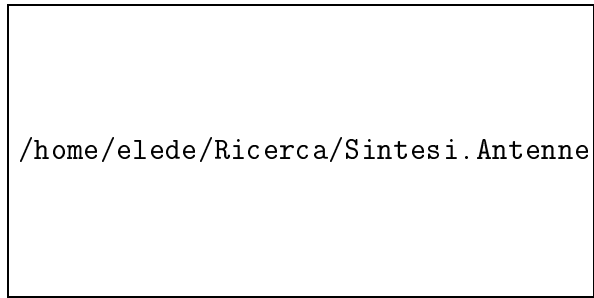


Figure 7 - R. Azaro *et al.*, "Synthesis of a pre-fractal dual-band monopolar ..."



(a)



(b)

Figure 8 - R. Azaro *et al.*, "Synthesis of a pre-fractal dual-band monopolar ..."